Journal of Materials Chemistry C

Accepted Manuscript

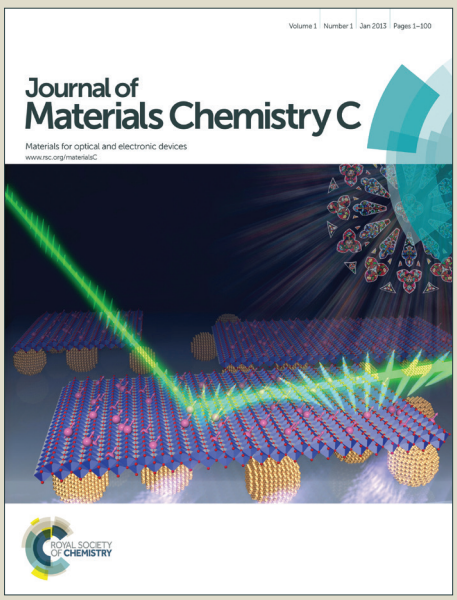

ROYAL SOCIETY OF CHEMISTRY

www.rsc.org/materialsC

Copper Nanowire Based Transparent Conductive Films with High Stability and Superior Stretchability

Yin Cheng, Shouling Wang, Ranran Wang, Jing Sun*, Lian Gao*

State Key Laboratory of High Performance Ceramics and Superfine Microstructure, Shanghai Institute of Ceramics, Chinese Academy of Sciences, Shanghai 200050, China

E-mail: wangranran@mail.sic.ac.cn, jingsun@mail.sic.ac.cn.

Abstract

In contrast to traditional "rigid and brittle" electronics, nowadays new electronic materials tend to be flexible, curvilinear, and even stretchable to meet the demands of wearable or body conformal electronic devices. Herein, a facile strategy has been demonstrated to synthesize copper nanowires with fewer particles and higher yield (promoted by 3 times). Through an artful fabrication and transfer technique, copper nanowires are constructed into stretchable conductive films, which not only possess good conductivity-transmittance performance (91% for 220 Ω/□), but also exhibit excellent mechanical robustness against adhesion, friction and bending. Besides, the partly-embedding structure of nanowire network gives rise to chemical resistance (stable conductivity through acid/alkali test), and most significantly, extremely superb stability against oxidation (no degradation of conductivity after 50 days in ambient condition). This work opens a way for Cu nanowire-based transparent conductive film into various practical applications, especially when harsh environmental conditions are inevitable.

1. Introduction

As an emerging research scope, stretchable electronics have been receiving ever-increasing attention from material scientists and engineers, which involves various applications such as skin sensors for robotics, implantable medical devices, wearable electronics and highly deformable optoelectronic products. For the realization of the devices above, a stretchable

electrode that is both transparent and electrically conductive is often demanded. The achievement of such electrodes mostly can be actualized through "materials that stretch" or "structure that stretch".[1] The former refers to conductive materials comprised of an elastic matrix embedded with conducting fillers, such as metal, carbon nanotubes or conducting polymers.[2-4] The latter describes a strategy in which thin films or conducting ribbons like carbon nanotubes, metal nanowires are configured into wavy or buckled form and upon tensile strain the buckled components release the prestored deformation to demonstrate desired stretchability.[5-8]

One of the key factors to achieve stretchable electrodes of high quality is the choice of conducting component. Carbon nanotubes, graphene, silver nanowires are most extensively researched and utilized as the conducting part due to their superior conductivity and intrinsically flexible feature to some extent. These alternatives have already gained considerable progress in stretchable electronics.[9-12] However, copper nanowires (CuNWs) as a promising one-dimensional nanomaterial have not received much research concentration in stretchable electronics. The difficulty mainly lies in the lack of efficient and facile synthetic methods for high quality CuNWs (high aspect ratio, good purity, superior dispersibility) and their tendency to oxidation in ambient environment. Considering that copper is 1000 times more abundant while 100 times less expensive than silver[13] and possesses a comparable conductivity with silver ($\sigma_{Ag}=6.30\times10^7$ S·m^{-1}, $\sigma_{Cu}=5.96\times10^7$ S·m^{-1}), CuNWs will obtain immense development in stretchable electronics if the aforementioned hurdles are overcome. Here we present a novel modification of an existing solvothermal method for CuNWs synthesis and the employment of the resultant high quality nanowires in the fabrication of stretchable composite electrodes. Platinum nanoparticles (Pt NP) of ~ 5 nm in diameter were synthesized as new catalyst to improve the quality and yield of CuNWs. Composite conducting films were obtained after transferring the CuNWs network from glass substrate to an elastic poly(acrylate) matrix through *in situ* photo polymerization. The final electrode

possesses good performance in terms of sheet resistance (R_{sh}) and transparency ($T_{15\ \Omega/\square}$ =80.03%). As the interpenetrating conducting network were partly embedded into the poly(acrylate) substrate, the resulting electrode was imparted not only stretch ability (ultimate strain up to 17%), but also mechanical robustness against tape test and acid/alkali resistance. Besides, the surface roughness of the conducting film decreased sharply after transfer. Most significantly, the composite electrode demonstrated excellent oxidative stability compared with the bare CuNW film on rigid substrate, which opens up opportunities for CuNW-based films into broad practical applications.

2. Results and Discussion

2.1. Synthesis of CuNWs

In a previous reported solvothermal method for CuNW synthesis,[14] hexadecylamine (HDA) and cetyltrimethylammonium bromide (CTAB) were mixed and heated to form a liquid-crystalline medium as tubular structure to realize the growth of CuNW, wherein a platinum sputtered Si wafer worked as catalyst. However, there are two disadvantages brought about by choosing the Pt sputtered Si wafer as catalyst. On the one hand, compared with nanoparticles as catalyst, the morphology of a sputtered Pt layer can hardly be adjusted, leaving much less room for tuning the diameter and length of nanowires, which is much easier to be accomplished through varying the concentration and diameter of nanoparticles as catalyst.[15] On the other hand, this involves a vacuum sputtering process, making it undesirable for all-solution synthetic strategy, which fits the scaling-up production better.

In our modified method, HDA and CTAB were mixed and heated to 180 ^{o}C to form a liquid-crystalline medium. Then the precursor, copper acetylacetonate [$Cu(acac)_2$], was added into the medium and the reaction system was incubated for a certain period of time. Thereafter, a certain amount of Pt nanoparticle solution was introduced to catalyze the growth of CuNW. After 12 hours reaction at 180^{o}C, CuNWs were synthesized with an average diameter of ~ 80

nm and length varying from tens to hundreds of micrometers. The modified method differs from the original one, including the step of incubation before adding the catalyst and the replacement of catalyst. Pt nanoparticles with diameters of 5 nm were formed by reducing $PtCl_2$ with ethylene glycol. In this so-called *polyol process*, ethylene glycol served as both solvent and reducing agent.[16] More information is provided in Supplementary Information. If the incubation procedure was absent, the final product contained large numbers of particles and the yield decreased obviously. The incubation step enabled the sufficient coordination of precursor molecules with Br^- and HDA, as indicated by a color change from dark green to light yellow gradually, thus enriching the metal moieties within the tubular channels. To figure out the influence of incubation time, 4mg Pt precursor, $PtCl_2$, was used for Pt NP synthesis and then 5μL of Pt NP suspension was introduced into the reaction system, the incubation time being 0.5h and 1.5h respectively. **Figure 1** showed the SEM images of the final product. As seen from Figure 1, with the incubation time increasing from 0.5 h to 1.5h, the number of particles around the nanowires increased notably, which means the prolongation of incubation time was undesired for high quality nanowire, for the particles would inevitably deteriorate the performance of the resulting CuNW-based thin film. According to more experimental trials with varying incubation time, 0.5 h was appropriate. A possible mechanism was figured out to explain this phenomenon: The Pt NP facilitated the electron transfer from reducing moieties (NH^{4+}) to Cu^{2+} and also worked as the seeds for heterogeneous nucleation of Cu atoms. When the incubation was absent or insufficient, the Pt NP initiated the nucleation of Cu atoms and growth into particles because of inadequate time for the formation of liquid crystal tubular templates. As incubation proceeded, the tabular templates were assembled and Cu^{2+} was coordinated with Br^- and HDA, which was in favor of nanowire synthesis. However, prolonged incubation at elevated temperature oxidized HDA, thus destroying the integrity of the soft templates, which caused particle formation. As a result, there existed an optimal incubation time and in this circumstance, being 0.5h.

For synthesis of metallic nanowire using seed-mediating method, the catalyzing seeds play a critical role in tuning the nanowire.[15, 17-19] We specifically investigated the influence of catalyst amount on the final product. Herein, when the amount of catalyst was on the order of milliliter, particles dominated the product. When the amount was less than 5μL from 2mg catalyst precursor, nanowires could not be synthesized successfully. To determine the optimal catalyst amount, we decreased the mount of Pt precursor, $PtCl_2$, from 4 to 3, 2 mg. Then, 5μL out of the catalyst suspension was taken out for synthesis. After that, the final products were characterized by SEM and TEM (**Figure 2**). As the Cu particles could unavoidably undermine the performance of the nanowire-based transparent conductive film, it is necessary to evaluate the proportion of the particles involved in the final nanowires. To quantitatively access the amount of particles in the nanowires, a reasonable evaluating method was proposed for the first time. We utilized typical TEM images for each sample and made a statistical calculation in terms of *the number of particles per nanowire and the number of particles per micrometer of nanowire.* The evaluation result is presented in Supplementary Information. With the help of the statistical results, it can be concluded easily that the optimal catalyst amount is 5 μL of Pt NP suspension from 2 mg Pt precursor.

To the best of our knowledge, it still remains a great challenge to synthesize high quality CuNWs (large aspect ratio, high purity, superior dispersibility) with a large yield through a facile method. Wiley *et al.*[20] scaled up a solution process method reported by Zeng *et al.*[21] by 200 times and therefore made Cu NWs possible for transparent electrode applications. In their work, over 1 g of Cu NWs was synthesized by solution processing. However, the synthesized nanowires led to nanowires with a significant amount of Cu particles and poor dispersibility, and the nanowires were still relatively short (an average length of ~ 10 μm). In our modified synthetic method, the typical yield of CuNWs was 0.015 g (conversion efficiency of copper element being 30.9 %), which is 3 times of that from the original synthesis. We further scaled the reaction by 5 times and the yield of final product was promoted to 0.08 g (conversion

efficiency of copper element being 33 %). The as-synthesized CuNWs possess superior dispersibility with an average diameter of ~ 90 nm and length from tens to hundreds of micrometers. More information about this is supplied in Supplementary Information.

2.2. Fabrication and performance of stretchable electrodes

With the high quality CuNWs, stretchable electrodes were fabricated in a novel way. First, a CuNW film was prepared on a glass substrate through vacuum filtration and hot-pressing transfer. Then liquid acrylate monomer solution was drop-cast onto the conducting film and a blank glass slide was put on top with a layer of adhesive tape in between as a thickness-controlling spacer. After ultraviolet irradiation and peeling off glass substrate, the CuNW network was transferred to the surface of the cured poly(acrylate) substrate, resulting in a transparent conductive composite film with a thickness of 50 μm (**Figure 3a**). The as-prepared film exhibited great flexibility (rolled up to a cylinder shape in **Figure 3b**), which would be investigated in later part. After being transferred, rare CuNWs could be found on the glass substrate. The surface morphology of the conducting network before and after the transfer was demonstrated in **Figure 3**. As seen from the optical images (**Figure 3c, 3d**), the interpenetrating network was partly embedded into the polyacrylate substrate. **Figure 3e** revealed the homogenous distribution of CuNWs on the glass slide. The SEM image (**Figure 3f**) further demonstrated the partly-embedding morphology of the network clearly. To evaluate the integrity of the conducting network during transfer, the R_{sh} of three samples were measured before and after the transfer operation. Three samples all showed a negligible change (< 5%) through transfer (3.2 Ω/□ to 3.4 Ω/□, 4.8 Ω/□ to 5.0 Ω/□, 15.2 Ω/□ to 15.7 Ω/□), indicating that the percolating nanowire network remained intact during the transfer operation.

In order to characterize their electrical and optical transmission properties, we fabricated a series of films with varying sheet resistance through controlling the thickness of the conducting CuNW network in the filtration step. **Figure 4** showed the optical transmittance

spectra (400 nm~ 800 nm) of composite films with varying sheet resistance. The composite electrodes have fairly high transparency performance. The transmittance is about 91.5% at 550 nm wavelength for a 220 Ω/□ electrode, 86.6% for a 72 Ω/□ electrode, 80% for 15 Ω/□, and 70.5% for 5 Ω /□. The results were comparable to or outperformed many other polymer substrate based TCF reported before.[22-25]

A smooth surface of the electrode is a critical requirement for its application in optoelectronic devices, especially for OLEDs and organic solar cells. Judging from the partly-embedding nature of the conducting network, the surface roughness of the composite films ought to be diminished compared with that before transfer. **Figure 5** shows the typical 3D AFM images of two films with different R_{sh} before and after the transfer operation. **Figures 5a** and **5c** are CuNW films on glass substrate with R_{sh} being 9.1 Ω/□ and 18.4 Ω/□, and their RMS surface roughness was 165.1 nm and 88.2 nm respectively. **Figures 5b** and **5d** are the corresponding composite films after transfer with R_{sh} being 9.3 Ω/□ and 19 Ω/□, and their RMS surface roughness was 71.3 nm and 18.7 nm respectively. Apparently, the transfer manipulation decreased the surface roughness of the films sharply. For OLEDs, 1-2 nm surface roughness is typically required.[26] This could be achieved by encapsulation of the composite electrode with conducting polymers to smooth the surface further more.

Except for a smooth surface, it also requires the functional stability against ambient environment for the practical application of transparent conductive electrodes. For CuNW-based electrodes, the oxidative stability is always the key issue researchers concern. Wiley[27] has greatly improved the resistance to oxidation of nanowire-based transparent electrodes by coating CuNWs with nickel. However, the coating operation also brought about problems of extra processing cost and impaired performance (lower transmittance at a given R_{sh}). In a recent work of Rodney S. Ruoff[28], reduced grapheme oxide platelets were deposited on top of Cu NWfilms to act as an oxidation resistant layer. Though the anti-oxidation ability was enhanced after deposition of reduced graphene oxide platelets, the effect was investigated and

confirmed in only 72h. Chemical vapor deposition graphene has also been employed as a protective layer upon Cu surface, unfortunately, this trial accelerated long-term oxidation of an underlying copper substrate in ambient atmosphere at room temperature ascribed to the intensified electrochemical corrosion process.[29,30] It is reasonable to infer that our composite films would be dramatically enhanced in anti-oxidation ability owing to the partly-embedding fact. In order to confirm this, we recorded the sheet resistance of the composite films and glass substrate- based films with similar R_{sh} as a contrast, with the temperature and relative humidity being 27 ^{o}C and 40 % respectively. The result is shown in **Figure 6**. For CuNW films on glass slide with R_{sh} of 10 Ω/□ and 30 Ω/□, the sheet resistance began to increase after just one day and rose by an order of magnitude after about 10 days. As a comparison, the sheet resistance of the corresponding composite films after transfer remained rather stable over a period of 50 days, the R_{sh} variation being so small as to be within the error of measurement. The polymer substrate could effectively insulate the CuNWs that were "underground" from the outer atmosphere. As for the CuNWs naked in air, more work needs to be done to explain why they were surprisingly stable as well.

As the oxidative stability was confirmed, we continued to test the chemical stability of the composite film against corrosive liquids, such as acid and alkali, to evaluate its application feasibility in harsh environment. Here, the standard industrial test for ITO was adopted to evaluate the acid and alkali resistance of the composite film. From the testing results (supplied in Supplementary Information), the R_{sh} increase of the composite film was reduced drastically to about 10% after the corrosion test compared with that before transfer. Obviously the burying of the Cu NWs under the surface of polyacrylate could effectively protect them from chemical attack by corrosive chemicals, which provide the possibility for their use in harsh environmental conditions.

Thanks to the mechanical compliancy of ultra-long CuNWs and the elasticity of the polymer substrate, the composite electrodes gained excellent flexibility and stretch ability. To assess

the electric conductivity during the stretching process, we performed tensile test to the films. The conducting film was cut into 10 mm × 30 mm strips and clamped by fixtures on universal testing machine with a constant tensile speed of 0.2 mm/min, while electric resistance was measured simultaneously. Figure 7a shows the first stretching process for three samples with different initial resistance. It can be seen for all the samples the resistance increased to about 2 times at the rupture strain of ~15% as compared with the original one. Figure 7b describes the resistance change of the first stretching/releasing cycle with a composite film of 5.8 Ω. The resistance increased from 5.8Ω to 12.7Ω somewhat linearly, and then recovered partially to 9.2Ω when the film was fully released. 0-10% stretching/releasing cycles were further carried out to a composite film of 5Ω for 20 times and the resistance at the strain of 0% and 10% were recorded. In Figure 7c the resistance increased after each stretching and recovered partly after each releasing, the general trend being nearly linear.

To unravel the mechanism underlying the phenomenon during stretching/releasing, SEM images of the conducting surface of films were taken before the first stretching and after the first releasing respectively, as seen in **Figure 8**. In **Figure 8 (a, c, e)**, the nanowires before stretching were distributed uniformly and oriented randomly. After the first stretching and releasing cycle, a preferred orientation of CuNWs along the stretching direction occurred as shown in **Figure 8 (b, d, f)**. In the SEM images of the released film, no obvious sign of nanowire fracture was found. Based on the above results, we proposed a sliding mechanism to explain the resistance change during stretching and releasing. As the composite film was stretched, the polymer matrix elongated and the bonding between the nanowires and polymer coerced the nanowires into sliding along the stretching axis. The originally intimate contacts between nanowires would undoubtedly get loosened as the sliding proceeded, which increased the contact resistance and resulted in the overall resistance increase of the stretched film. Upon releasing, the contraction of polymer matrix tightened the contacts between nanowires again, though not enough to reach the original state before stretching, accounting

for the partly recovered conductivity of the composite film. This sliding mechanism was also found in a recently reported paper.[31]

The burying of the nanowires at the surface of poly (acrylate) also gives the composite film the advantage of mechanical robustness against adhesion, friction, and bending. To know the mechanical stability of the composite film, tape test and friction test were carried out. As a comparison, the glass substrate-based films with similar R_{sh} were tested at the same time. In the tape test, an ordinary adhesive-tape was attached to the conducting surface and peeled off. Consequently, the CuNW network on the glass slide was peeled away directly and lost the conductivity. While the composite film kept intact and the sheet resistance increased from 3.2 Ω /□ to 3.4 Ω /□, testifying their great mechanical robustness against adhesive force. When friction was applied on the conducting surface, the conducting network on the glass slide was destroyed, while the composite film displayed no measurable R_{sh} increase. More details can be attained in Supplementary Information. We further tested the sheet resistance change of the composite films when they (10 mm × 30 mm strips) were bended along the longer side to a semi-circle repeatedly. More specifically, we imposed tensile and compressive bending respectively on the conducting surface cyclically. **Figure 7d** records the sheet resistance of films after cyclical bending. The R_{sh} of composite films changed little even after 1000 times of tensile and compressive bending, exhibiting superior stability against bending deformation. This result outperforms an AgNW-PVA composite film reported before, wherein the resistance increased by 2–3 times only after 250 cycles of tensile or compressive folding.[32]

3. Experimental

Synthesis of platinum nanoparticles: The synthetic method was based on a polyol process reported before.[33] A certain amount of $PtCl_2$ (2, 3, 4 mg) was dissolved into 1ml ethylene glycol and then added into a round-bottom flask with 2ml ethylene glycol heated to 160 ^oC in an oil bath. The flask was equipped with a condenser pipe and a magnetic stirring bar to keep

the reaction under continuous stirring. 3 mL of gray black suspension containing platinum nanoparticles were collected from the flask after about 3 min. 5 μL out of the as-prepared 3 mL suspension containing platinum nanoparticles was used as catalyst within half an hour before obvious sedimentation occurred.

Synthesis of CuNWs: For CuNW synthesis, we modified an existing solvothermal method already reported by our research team.[13] A typical synthesis process is as follows. First, 8 g hexadecylamine (HDA) and 0.5 g cetyltrimethylammonium bromide (CTAB) were mixed in a glass vial and melted at 180 ^{o}C to form a homogeneous solution. Then, 0.2 g copper acetylacetonate [Cu(acac)2] was added into the above solution with mild agitation. In the previous method, a platinum sputtered Si wafer was introduced into the reaction system right after the copper salt was dissolved. However, in the modified one, after the addition of copper salt, the glass vial was kept under 180 ^{o}C for a certain time of incubation (0.5, 1h). After the incubation procedure, 5 μL of as-prepared platinum nanoparticle solution was dropped into the reaction system with a pipette, followed by 12h reaction at 180 ^{o}C. When the synthetic reaction was over, the product was rinsed with toluene for several times and a brownish red CuNW blanket was obtained at last. The as-synthesized CuNWs were preserved in toluene for use. For the scale-up synthesis, the usage amount of all the reaction reagents and catalyst were amplified by 5 times.

Fabrication of composite electrode: The fabrication of composite electrode involved two main steps.[33] One was to prefabricate a CuNW film onto a glass substrate, and the other was to transfer the CuNW film onto an elastic poly(acrylate) matrix through in situ photo polymerization. In the fabrication of glass substrate-based CuNW film, typically, a slight amount of Cu NWs was dispersed in toluene. Then the suspension containing Cu NWs was vacuum-filtrated onto a nitrocellulose filter membrane. After that, the filter membrane was transferred onto a glass slide through hot-pressing at 80 ^{o}C in vacuum for 1h, and then dipped into acetone for ~30 min to dissolve the filtration membrane, leaving a Cu NW film on the

glass slide. At last, the glass slide with film on it was treated in in H_2 at 300 ^oC for 1h to remove oxide layer and the residual HDA on the surface of Cu NWs. In the transfer process, first, an acrylate monomer solution was prepared: a dimethacrylate (SR540, Sartomer USA LLC) and a low-viscosity aromatic monoacrylate (CN131, Sartomer USA LLC) were mixed at the weight ratio of 1:3, and a photoinitiator, 2,2-dimethoxy-2-phenylacetophenone was dissolved in the liquid monomer solutions at 1 wt% concentration. The liquid monomer solution was drop-cast over the CuNW film on a glass slide and then covered a blank glass slide with a layer of adhesive tape in between as the spacer to control the thickness of the monomer solution. The liquid monomer was subsequently cured under ultraviolet irradiation, resulting in a composite film which could be peeled off from the glass substrate easily.

Characterization: Scanning electron microscopic images were taken using a Hitachi S-4800 FE-SEM. The CuNWs were characterized by SEM without further centrifugation after synthesis. The transmission electron microscopic images were taken with a JEOL 200CX electron microscope. For platinum nanoparticle characterization, the sample was prepared by dipping a copper grid into the Pt nanoparticle suspension and dried at room temperature. To determine the yield of Cu NW, the final product was dried in vacuum after rinsing and weighed. The electric resistance of composite electrode was measured with a digital multimeter (VICTOR DT930F+). The sheet resistance was obtained through a Loresta-EP MCP-T360 (Mitsubishi Chemical Corporation). The transmittance spectrum was taken with a UV/VIS Spectrometer (Lambda 950, Perkin Elmer). The tensile test of the composite films was performed on an Instron-1195 tester. The surface roughness of the composite film was measured with an atomic force microscope.

4. Conclusion

We have successfully improved the quality and yield of CuNWs by modifying a solvothermal synthetic strategy and demonstrated the utilization of the high-quality nanowires for

composite stretchable electrodes with excellent performance detailedly. The purity of CuNWs could be controlled through adjusting the amount of catalyst and the yield was promoted notably. The composite transparent conductive film shows a typical sheet resistance of 220 Ω/□ at 91.5 % transparency, which compares favorably with other composite transparent electrodes. These films possessed good flexibility and stretchability owing to the combination of elastic substrate and highly flexible Cu NWs with high aspect ratio. Compared with the glass-substrate films, the composite films are fairly superior in mechanical robustness and chemical stability (especially oxidative stability). We believe, with the advantage of low cost, the superb integrated performance of the films paves the way for their exploitation into the realm of stretchable electronics, such as wearable optoelectronic devices, body-conformal sensors, and human-implantable medical devices. The investigation of the composite films into practical application is underway.

Acknowledgements
This work was fincially supported by the National Basic Research Program of China (2012CB932303), the National Natural Science Foundation of China (Grant No.61301036)**,** Shanghai Municipal Natural Science Foundation (Grant No. 13ZR1463600 and 13XD1403900) and The Innovation Project of Shanghai Institute of Ceramics.

Electronic Supplementary Information (ESI) available: more information mentioned in the paper is available in Supplementary Information. See DOI: 10.1039/b000000x/

Notes and references

[1] J. A. Rogers, T. Someya, Y. Huang, *Science,* 2010, **327**, 1603.

[2] T. Sekitani, Y. Noguchi, K. Hata, T. Fukushima, T. Aida, T. Someya, *Science,* 2008, **321**, 1468.

[3] K. Y. Chun, Y. Oh, J. Rho, J. H. Ahn, Y. J. Kim, H. R. Choi, S. Baik, *Nat. Nanotechnol.* , 2010, **5**, 853.

[4] A. C. Siegel, D. A. Bruzewicz, D. B. Weibel, G. M. Whitesides, *Adv. Mater.,* 2007, **19**, 727.

[5] D. H. Kim, J. H. Ahn, W. M. Choi, H. S. Kim, T. H. Kim, J. Song, Y. Huang, Z. Liu, C. Lu, J. A. Rogers, *Science,* 2008, **320**, 507.

[6] D. J. Lipomi, M. Vosgueritchian, B. C. Tee, S. L. Hellstrom, J. A. Lee, C. H. Fox, Z. Bao, *Nat. Nanotechnol.,* 2011, **6**, 788.

[7] F. Xu, Y. Zhu, *Adv. Mater.,* 2012, **24**, 5117.

[8] Y. Zhu, F. Xu, *Adv. Mater.,* 2012, **24**, 1073.

[9] C. Yu, C. Masarapu, J. Rong, B. Wei, H. Jiang, *Adv. Mater.,* 2009, **21**, 4793.

[10] K. S. Kim, Y. Zhao, H. Jang, S. Y. Lee, J. M. Kim, K. S. Kim, J. Ahn, P. Kim, J. Choi, B. H. Hong, *Nature,* 2009, **457**, 706.

[11] P. Lee, J. Lee, H. Lee, J. Yeo, S. Hong, K. H. Nam, D. Lee, S. Lee, S. H. Ko, *Adv. Mater.,* 2012, **24**, 3326.

[12] W. Hu, X. Niu, L. Li, S. Yun, Z. Yu, Q. Pei, *Nanotechnology,* 2012, **23**, 344002.

[13] L. Hu, H. Wu, Y. Cui, *MRS Bull*, 2011, **36**, 760.

[14] D. Zhang, R. Wang, M. Wen, D. Weng, X. Cui, J. Sun, H. Li , Y. Lu, *J. Am. Chem. Soc.,* 2012, **134**, 14283.

[15] D. Azulai, E. Cohen, G. Markovich, *Nano Lett.,* 2012, **12**, 5552.

[16] Y. Sun, Y. Yin, B. T. Mayers, T. Herricks, Y. Xia, *Chem. Mat.,* 2002, **14**, 4736.

[17] N. R. Jana, L. Gearheart, C. J. Murphy, *J. Phys. Chem. B,* 2001, **105**, 4065.

[18] K. Zou, X. H. Zhang, X. F. Duan, X. M. Meng, S. K. Wu, *J. Cryst. Growth,* 2004, **273**, 285.

[19] A. Gole, C. J. Murphy, *Chem. Mat.,* 2004, **16**, 3633.

[20] A. R. Rathmell, S. M. Bergin, Y. L. Hua, Z. Y. Li, B. J. Wiley, *Adv. Mater.,* 2010, **22**, 3558.

[21] Y. Chang, M. L. Lye, H. C. Zeng, *Langmuir,* 2005, **21**, 3746.

[22] Z. Yu, X. Niu, Z. Liu, Q. Pei, *Adv. Mater.,* 2011, **23**, 3989.

[23] S. De, P. E. Lyons, S. Sorel, E. M. Doherty, P. J. King, W. J. Blau, N. Peter, J. Boland, V. Scardaci, J. N. Coleman, *ACS Nano,* 2009, **3,** 714.

[24] V. C. Tung, L. M. Chen, M. J. Allen, J. K. Wassei, K. Nelson, R. B. Kaner, Y. Yang, *Nano Lett.,* 2009, **9**, 1949.

[25] I. N. Kholmanov, M. D. Stoller, J. Edgeworth, W. H. Lee, H. Li, J. Lee, C. Barnhart, J. Potts, R. Piner, R. S. Ruoff, *ACS Nano,* 2012, **6**, 5157.

[26] K. Müllen, U. Scherf, *Organic Light Emitting Devices: Synthesis, Properties and Applications*, Wiley-VCH Verlag, Weinheim, Germany 2006.

[27] A. R. Rathmell, M. Nguyen, M. Chi, B. J. Wiley, *Nano Lett.,* 2012, **12**, 3193.

[28] I. N. Kholmanov, S. H. Domingues, H. Chou, X. Wang, C. Tan, J. Y. Kim, H. Li, R. Piner, A. Zarbin, R. S. Ruoff, *ACS Nano,* 2013, **7,** 1811.

[29] F. Zhou, Z. Li, G. J. Shenoy, L. Li, H. Liu, *ACS Nano,* 2013, **7**, 6939.

[30] M. Schriver, W. Regan, W. J. Gannett, A. M. Zaniewski, M. F. Crommie, A. Zettl, *ACS Nano,* 2013, **7**, 5763.

[31] B. J. Wiley, J. Zang, A. Rathmell, J. Wu, X. Zhao, *Nano Lett.,* 2013, **13**, 2381.

[32] X. Y.Zeng, Q. K. Zhang, R. M. Yu, C. Z. Lu, *Adv. Mater.,* 2010, **22**, 4484.

[33] Y. Sun, B. Gates, B. Mayers, Y. Xia, *Nano Lett.,* 2002, **2,** 165.

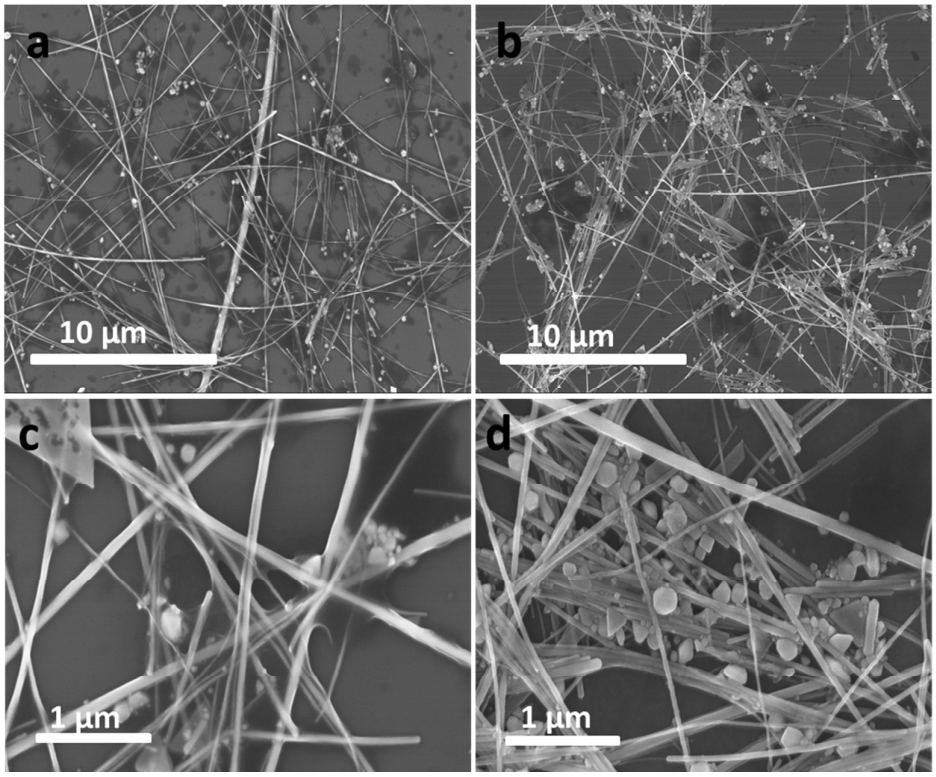

Figure 1. SEM images of CuNWs synthesized under different incubation time: (a, c) incubation time of 0.5 h; (b, d) incubation time of 1.5 h.

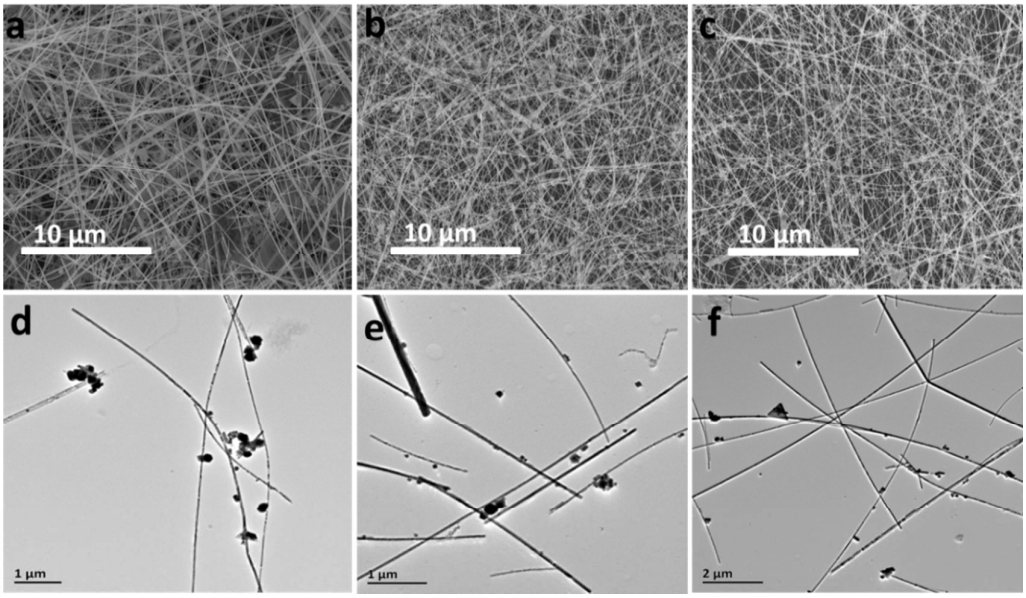

Figure 2. SEM and TEM images of CuNWs synthesized with different amount of Pt precursor ($PtCl_2$): (a, d) 4 mg. (b, e) 3 mg. (c, f) 2mg.

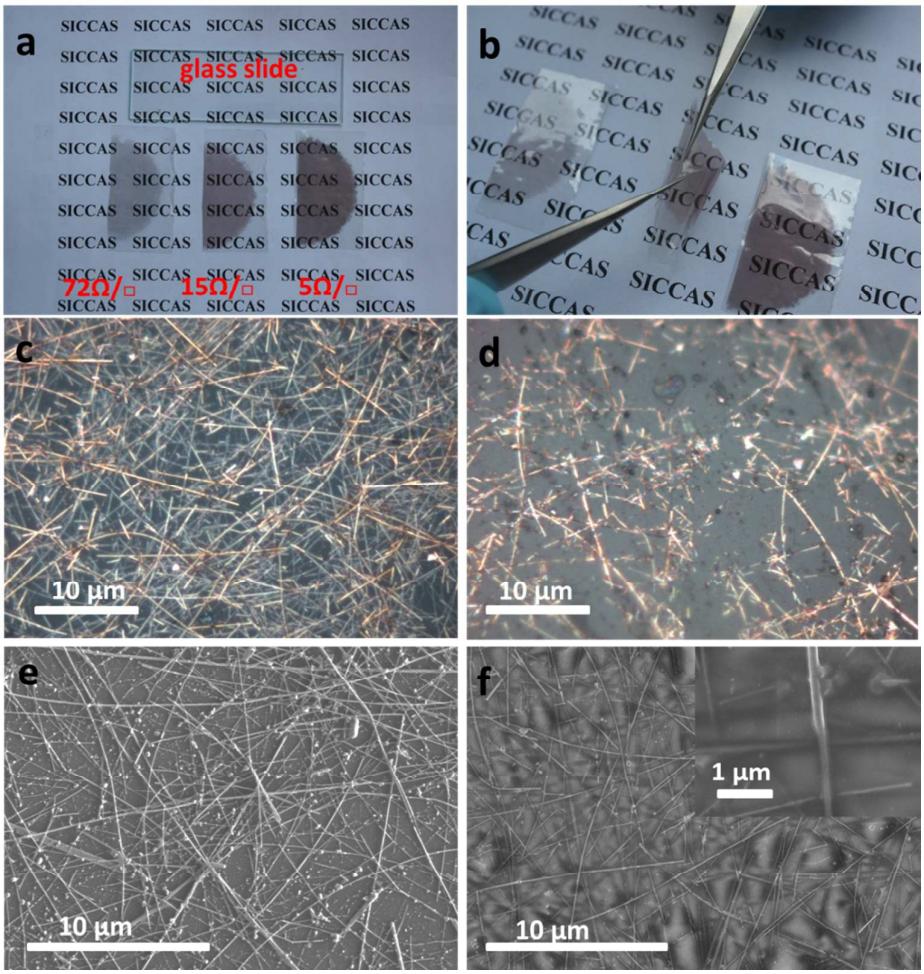

Figure 3. (a) Photos of composite films with varying sheet resistance. (b) A 15 Ω/□ composite film was rolled to a cylinder shape to demonstrate the great flexibility. Optical microscope images of conducting film of 15 Ω/□ on a glass slide (c) and after transfer (d). SEM images of CuNW films before (e) and after (f) transfer, corresponding to films in (c) and (d) respectively. The upper-right image in (f) was a higher magnification SEM picture to show detail information.

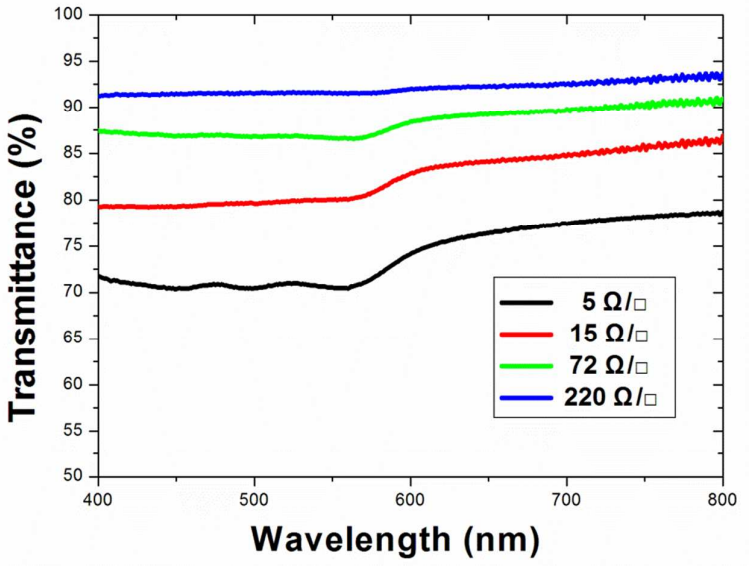

Figure 4. Transmittance spectra (400 nm~ 800 nm) of CuNW composite films with sheet resistance specified.

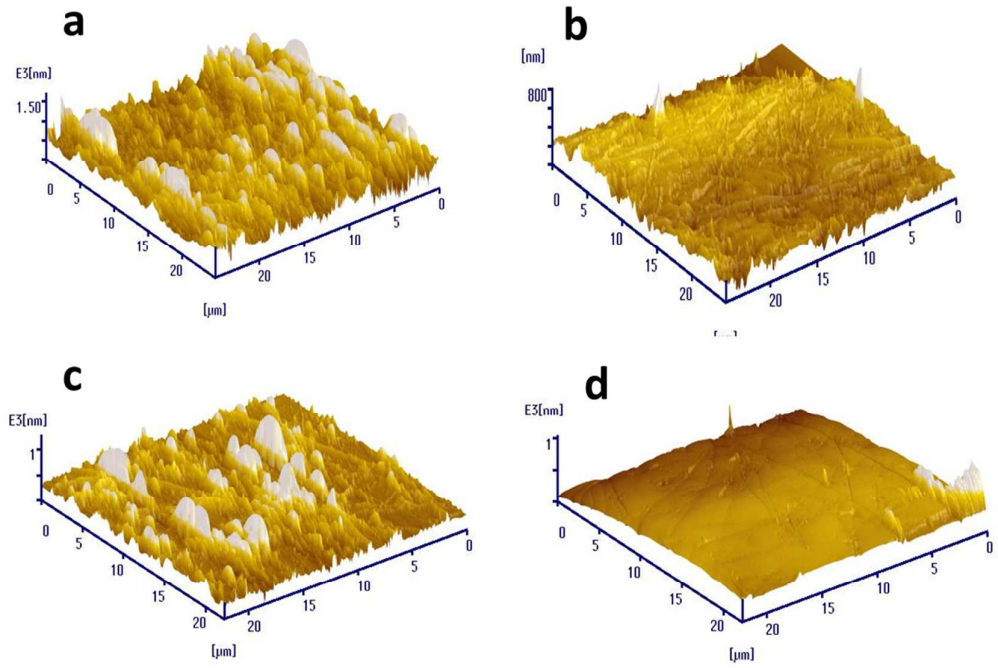

Figure 5. 3D AFM images of films before (a, c) and after (b, d) the transfer with varying initial sheet resistance: Rsh(a)=9.1 Ω/□, Rsh(c)=18.4 Ω/□.

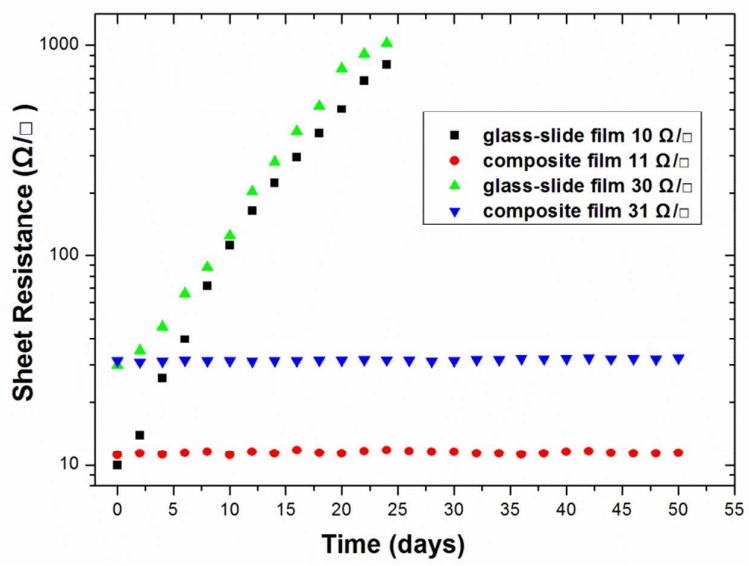

Figure 6. Sheet resistance vs time for CuNW films on glass slide and polymer substrate with similar initial R_{sh}. All the films were stored under room condition: temperature of 27 ^{o}C, relative humidity of 40 %.

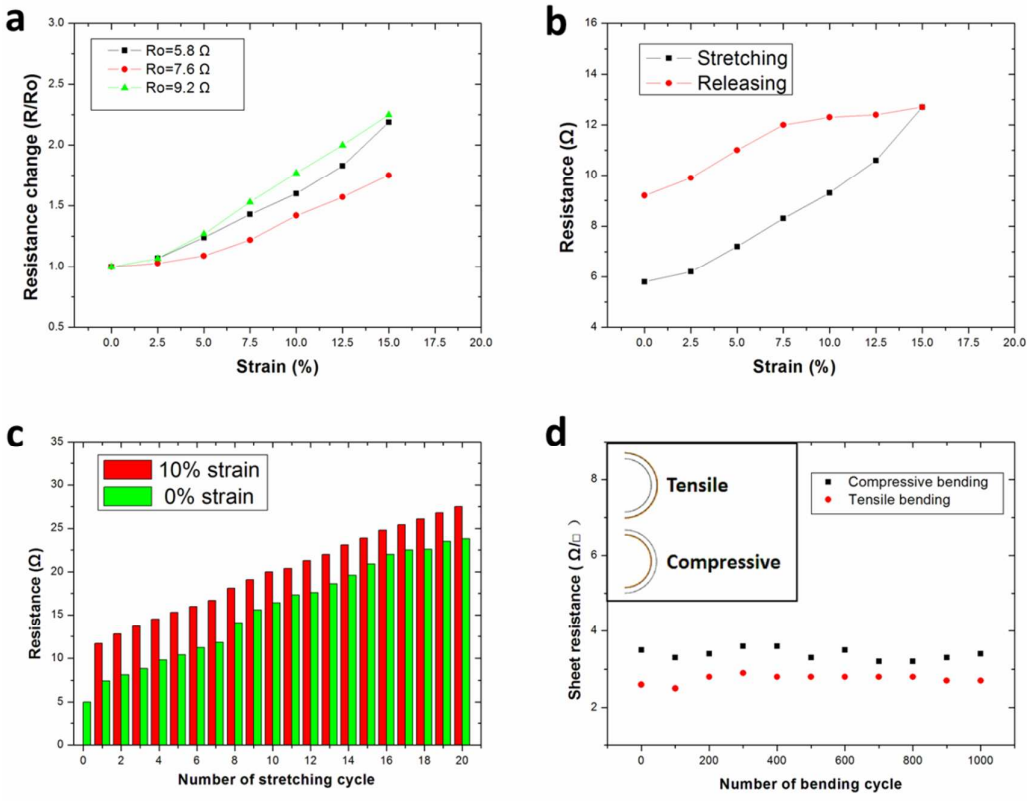

Figure 7. (a) Relative resistance change (R/Ro) of composite films with varying initial R_o during stretching. (b) Resistance change (Ro=5.8 Ω) during the first stretching and releasing cycle. (c) Resistance change for a 5 Ω composite electrode being cycled between 0% and 10%

strain for 20 times. (d) Change of Sheet Resistance of composite electrodes during cyclical tensile (2.6 Ω/□) and compressive (3.5 Ω/□) bending.

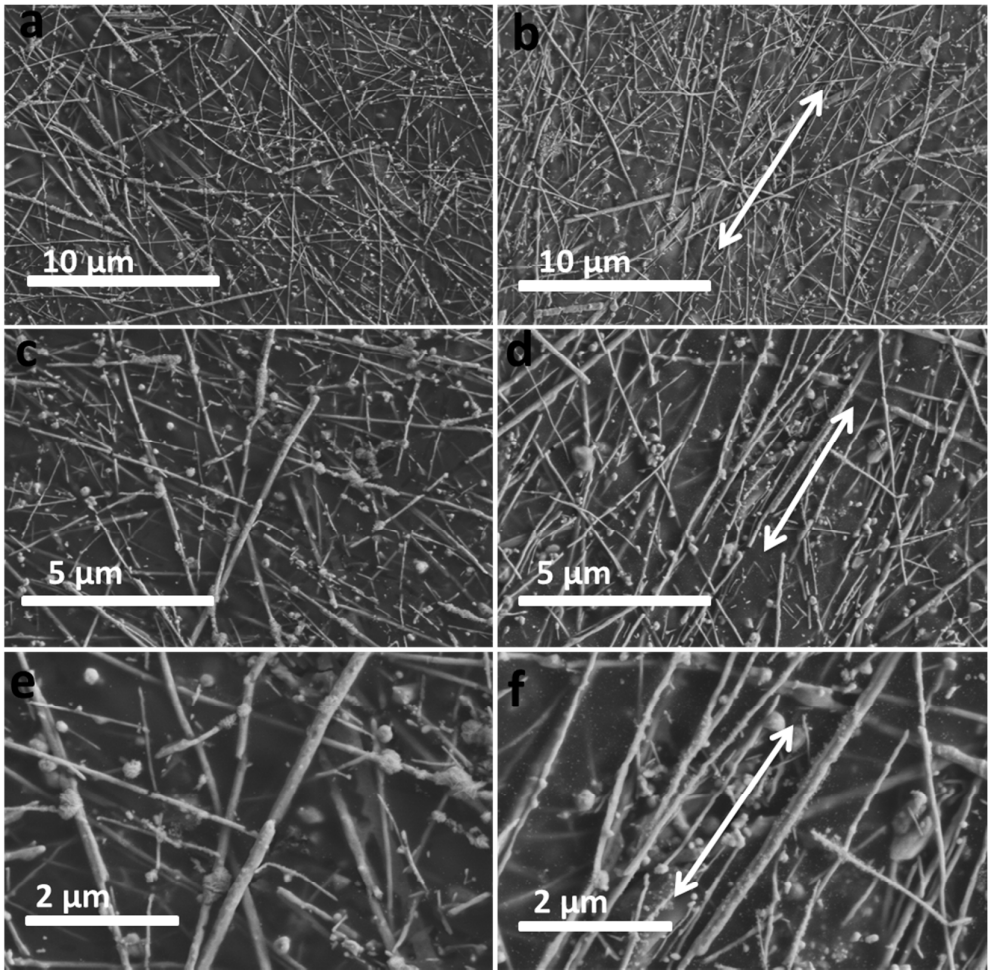

Figure 8. SEM images of the surface of a 7.6 Ω film before stretching with varying magnification (a, c, e). SEM images of the surface after the first releasing with corresponding magnification (b, d, f). The double-headed arrows in (b, d, f) mark the preferred orientation of copper nanowires.

TOC

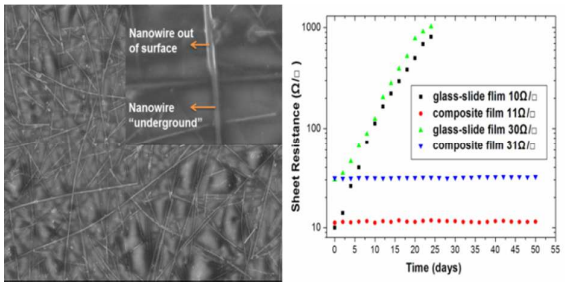

The unique partly-embedding structure imparts the copper nanowires based films as a transparent conductive electrode, not only with mechanical robustness but also great anti-oxidation stability.